nature materials

SUPPLEMENTARY INFORMATION

DOI: 10.1038/NMAT4492

Strong interplay between stripe spin fluctuations, nematicity and superconductivity in FeSe

Qisi Wang[1], Yao Shen[1], Bingying Pan[1], Yiqing Hao[1], Mingwei Ma[2], Fang Zhou[2], P. Steens[3], K. Schmalzl[4], T. R. Forrest[5], M. Abdel-Hafiez[6,7], Xiaojia Chen[6], D. A. Chareev[8], A. N. Vasiliev[9,10,11], P. Bourges[12], Y. Sidis[12], Huibo Cao[13] and Jun Zhao[1,14*]

[1] *State Key Laboratory of Surface Physics and Department of Physics, Fudan University, Shanghai 200433, China*

[2] *Beijing National Laboratory for Condensed Matter Physics, Institute of Physics, Chinese Academy of Science, Beijing 100190, China*

[3] *Institut Laue-Langevin, 71 Avenue des Martyrs, 38042 Grenoble Cedex 9, France*

[4] *Juelich Centre for Neutron Science JCNS Forschungszentrum Juelich GmbH, Outstation at ILL, 38042 Grenoble, France*

[5] *European Synchrotron Radiation Facility, BP 220, F-38043 Grenoble Cedex, France*

[6] *Center for High Pressure Science and Technology Advanced Research, Shanghai, 201203, China*

[7] *Faculty of Science, Physics Department, Fayoum University, 63514 Fayoum, Egypt*

[8] *Institute of Experimental Mineralogy, Russian Academy of Sciences, 142432 Chernogolovka, Moscow District, Russia*

[9] *Low Temperature Physics and Superconductivity Department, M.V. Lomonosov Moscow State University, 119991 Moscow, Russia*

[10] *Theoretical Physics and Applied Mathematics Department, Ural Federal University, 620002 Ekaterinburg, Russia*

[11] *National University of Science and Technology "MISiS", Moscow 119049, Russia*

[12] *Laboratoire Leon Brillouin, CEA-CNRS, CEA-Saclay, 91191 Gif sur Yvette, France*

[13] *Neutron Scattering Science Division, Oak Ridge National Laboratory, Oak Ridge, Tennessee 37831-6393, USA*

[14] *Collaborative Innovation Center of Advanced Microstructures, Fudan University, Shanghai 200433, China*

I. X-ray single crystal diffraction refinements

To determine the chemical composition and crystalline structure of our FeSe crystals, we have performed X-ray diffraction measurements on a crystal from the same batch as those measured with neutrons using a Bruker D8 VENTURE Single Crystal X-ray Diffractometer. The Rietveld refinement was performed using the FULLPROF program[1]. The refined parameters are summarized in STable I.

II. Instrument configurations for the elastic and inelastic neutron scattering experiments

The elastic neutron diffraction on FeSe single crystals was measured on the 4F2 cold triple axis spectrometer at the Laboratoire Leon Brillouin, France and HB-3A four-circle diffractometer at the High Flux Isotope Reactor at Oak Ridge National Laboratory, United States[2]. The inelastic neutron scattering measurements were carried out on the IN20 thermal triple axis spectrometer at the Institut Laue-Langevin,

DOI: 10.1038/NMAT4492

Grenoble, France, and the 2T1 thermal triple axis spectrometer at the Laboratoire Leon Brillouin, France. For the measurements performed on IN20 (Figs. 2b-2e, 3a, 3b, and 4b), we used a focusing Si(111) as monochromator and a pyrolytic graphite [PG(002)] as analyzer. This setup yielded an energy resolution of about 1 meV at (1, 0, 0) at $E = 0$ meV. For the measurements performed on 2T1 (Fig. 3a), PG(002) was used as the monochromator and analyzer. A PG filter was installed in front of the analyzer to eliminate the contamination from the higher-order neutrons. A correction was also made for monitor contamination by higher-order neutrons. For both triple axis spectrometers, the final neutron energy was fixed at E_f=14.7 meV and no collimation was used.

III. Raw data, background subtraction and absolute units normalization

For typical inelastic neutron scattering experiments, the background is momentum, energy and temperature dependent. SFig. 1 shows several representative raw **Q**-scans measured at various temperatures. Each **Q**-scan can be fitted by a single Gaussian peak on a linear background. The data presented in Fig. 2 are obtained by subtracting the linear background from the raw **Q**-scans.

SFig. 2 shows the temperature difference of several **Q**-scans $[S(1.5K) - S(11K)]$ at 4 meV near the first Brillouin zone center (1, 0, 0), and the second Brillouin zone center (2, 1, 0). The 2D contour plot in Fig. 2e was interpolated from a series of such **Q**-scans.

SFig. 3 summarizes the raw energy scans at 1.5 K, 11 K and 110 K. The background was estimated as the average intensity at **Q** = (0.944, 0.330, 0) and **Q** = (0.944, −0.330, 0). The background-subtracted data are presented in Fig. 3.

SFig. 4a shows the temperature dependence of the signal at [**Q**=(1, 0, 0)] and background positions at 2.5 meV. As expected, the scattering intensity of the background decreases gradually with decreasing temperature. Nevertheless, on cooling to below T_s=90 K, a sudden increase of the scattering intensity at the signal is clearly seen (SFig. 4a). Similar behavior is also observed near T_c = 8.7 K at 4 meV (SFig. 4b).

The absolute units of the imaginary part of the dynamic susceptibility $\chi''(\mathbf{Q},\omega)$ (Fig. 3b) were calculated by comparing the intensity of spin fluctuations with that of the acoustic phonons. This approach has been used to normalize the spin fluctuation intensity in several iron based superconductors[3–5] and is intensively discussed in ref. 6. The integrated resonance spectral weight in FeSe is larger than that of $BaFe_{1.85}Ru_{0.15}As_2$ (T_c=14 K) and LiFeAs (T_c=16.4 K), but smaller than in $BaFe_{1.85}Co_{0.15}As_2$ (T_c=25 K).

IV. The evolution of the structural order parameter as a function of temperature. SFig. 5 shows

STable I: Refined structure parameters and chemical composition for tetragonal FeSe at T = 298 K. Space group: $P4/nmm$ (No. 129). Atomic positions: Fe: 2a (0, 0, 0); Se: 2c (0, 0.5, z).

	Refined composition	$FeSe_{0.990(10)}$
	a (Å)	3.7634(15)
	c (Å)	5.508(3)
Fe atom	B_{xx} (Å^2)	0.0219(15)
	B_{yy} (Å^2)	0.0219(15)
	B_{zz} (Å^2)	0.0482(18)
Se atom	z	0.2665(3)
	B_{xx} (Å^2)	0.0236(13)
	B_{yy} (Å^2)	0.0236(13)
	B_{zz} (Å^2)	0.0402(13)
	R_1	0.0566
	wRF^2	0.138
	χ^2	6.69

the temperature dependence of (4, 0, 0)/(0, 4, 0) structure peak. The peak splits below T_s=90 K. A weak anomaly is observed below T_c, which could be due to the competition between the nematicity and superconductivity.

*Correspondence and requests for materials should be addressed to J.Z. (zhaoj@fudan.edu.cn).

References

[1] Rodrguez-Carvajal, J. Recent advances in magnetic structure determination by neutron powder diffraction. *Physica (Amsterdan)*, **192B**, 55 (1993).

[2] Chakoumakos, B. C. et al. Four-circle single-crystal neutron diffractometer at the High Flux Isotope Reactor. *J. Applied Cryst.*, **44**, 655 (2011).

[3] Inosov D. S. et al. Normal-state spin dynamics and temperature-dependent spin-resonance energy in optimally doped $BaFe_{1.85}Co_{0.15}As_2$. *Nature Phys.* **6** 178-181 (2010).

[4] Zhao, J. et al. Effect of electron correlations on magnetic excitations in the isovalently doped iron-based superconductor $Ba(Fe_{1-x}Ru_x)_2As_2$. *Phys. Rev. Lett.* **110**, 147003 (2013).

[5] Qureshi, N. et al. Fine structure of the incommensurate antiferromagnetic fluctuations in single-crystalline LiFeAs studied by inelastic neutron scattering. *Phys. Rev. B* **90**, 144503 (2014).

[6] Xu, G. Y., Xu, Z. J. & Tranquada J. M. Absolute cross-section normalization of magnetic neutron scattering data. *Rev. Sci. Instrum.*, **84**, 083906 (2013).

DOI: 10.1038/NMAT4492

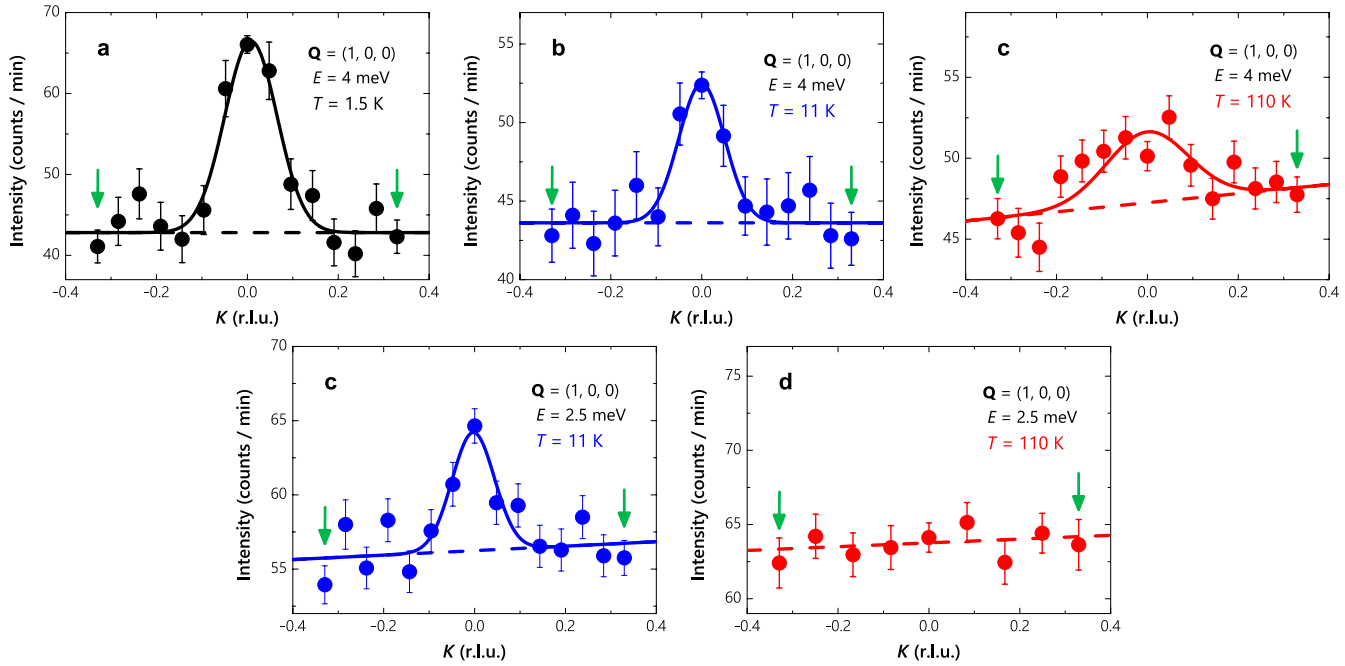

SFig 1: **Representative raw Q-scans measured at various temperatures in FeSe**. The **Q**-scan can be fitted by a single Gaussian peak on a linear background. The dashed line indicates the background. The background for E-scans is measured at **Q** = (0.944, ±0.330, 0) (green arrows). **a**, Rocking scan at E=4 meV, Q=(1, 0, 0), T=1.5 K. **b**, Rocking scan at E=4 meV, **Q**=(1, 0, 0), T=11 K. **c**, Rocking scan at E=4 meV, **Q**=(1, 0, 0), T=110 K. **d**, Rocking scan at E=2.5 meV, **Q**=(1, 0, 0), T=11 K. **e**, Rocking scan at E=2.5 meV, **Q**=(1, 0, 0), T=110 K.

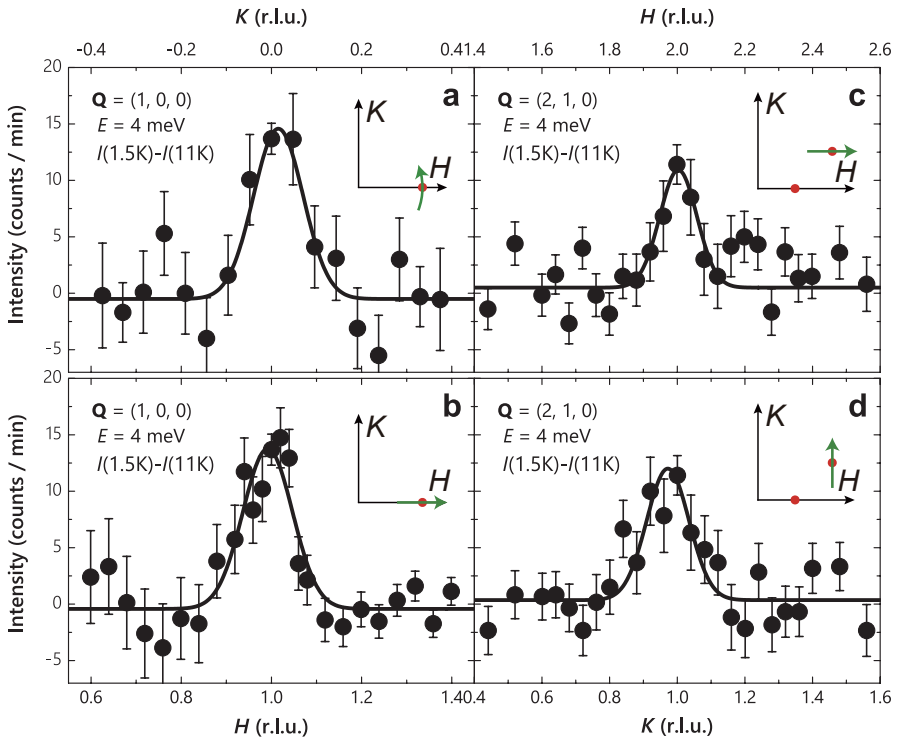

SFig 2: **Representative temperature difference Q-scans [S(1.5K) - S(11K)] at 4 meV near (1, 0, 0) and (2, 1, 0)**. The 2D contour plot in Fig. 2e was interpolated from a series of such **Q**-scans. The scan directions are marked in the insets. Each scan can be fitted by a single Gaussian peak. No significant anisotropy of the peak width is observed. **a**, Rocking scan at E=4 meV, Q=(1, 0, 0). **b**, Hscan at E=4 meV, Q=(1, 0, 0). **c**, Hscan at E=4 meV, Q=(2, 1, 0). **d**, Kscan at E=4 meV, Q=(2, 1, 0).

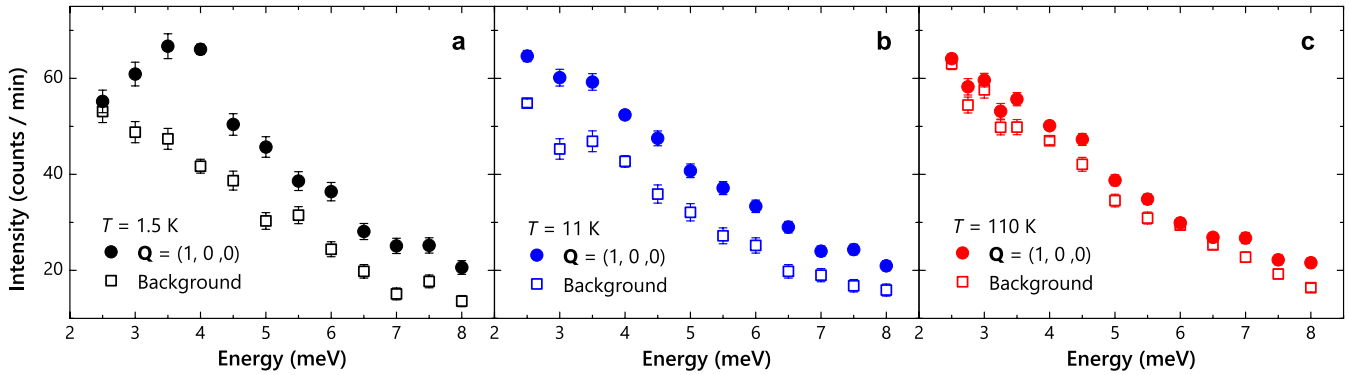

SFig 3: **Energy dependence of the scattering at the signal [Q=(1, 0, 0)] and background positions**. The background was estimated as the average intensity at **Q** = (0.944, 0.330, 0) and **Q** = (0.944, −0.330, 0), which are marked by green arrows in SFig.1. **a**, T=1.5 K. **b**, T=11 K. **c**, T=110 K. The overall magnetic spectral weight is clearly enhanced on cooling from 110 K to 11 K at the energies measured.

DOI: 10.1038/NMAT4492

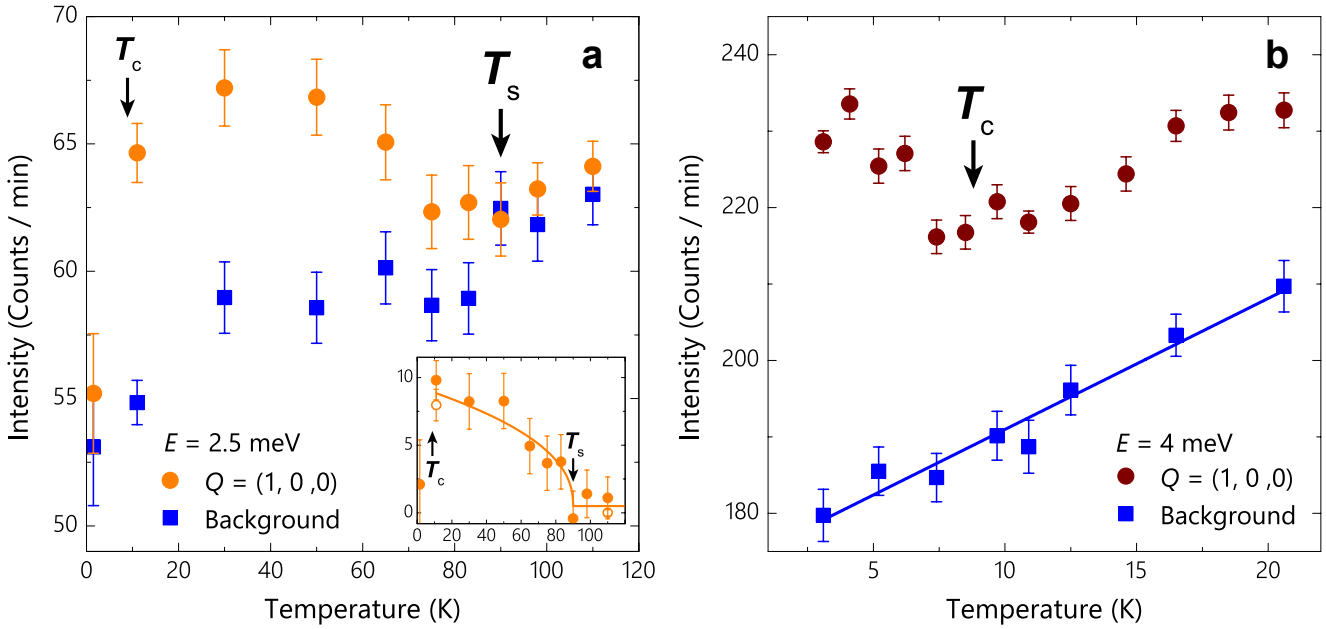

SFig 4: **Temperature dependence of the scattering at the signal [Q=(1, 0, 0)] and background positions at** 2.5 **meV and** 4 **meV**. The background-subtracted data are presented in Fig. 4. **a**, Temperature dependence of the scattering at the signal [**Q**=(1, 0, 0)] and background at 2.5 meV. The background was estimated as the average intensity at **Q** = (0.944, 0.330, 0) and **Q** = (0.944, −0.330, 0). Although the background decreases gradually with decreasing temperature, the signal exhibits a sudden increase at T_s=90 K. The inset shows the background-subtracted data. The open circles are data fitted with **Q**-scans. We note that the decrease of the scattering intensity at the signal at 1.5 K is simply due to the opening of the superconducting spin gap. **b**, Temperature dependent data for 4 meV with the background measured at **Q**=(1, 1, 0) and **Q**=(1, -0.6, 0). Since this scan was measured in a relatively narrow temperature range (3K to 21K), the background was estimated by a linear fitting of the data points collected at eight temperatures (blue squares). This is justified as most data points fall on the fitting curve (blue solid line). The data presented in SFig. 4b were collected on 2T1. All other inelastic neutron scattering data were collected on IN20.

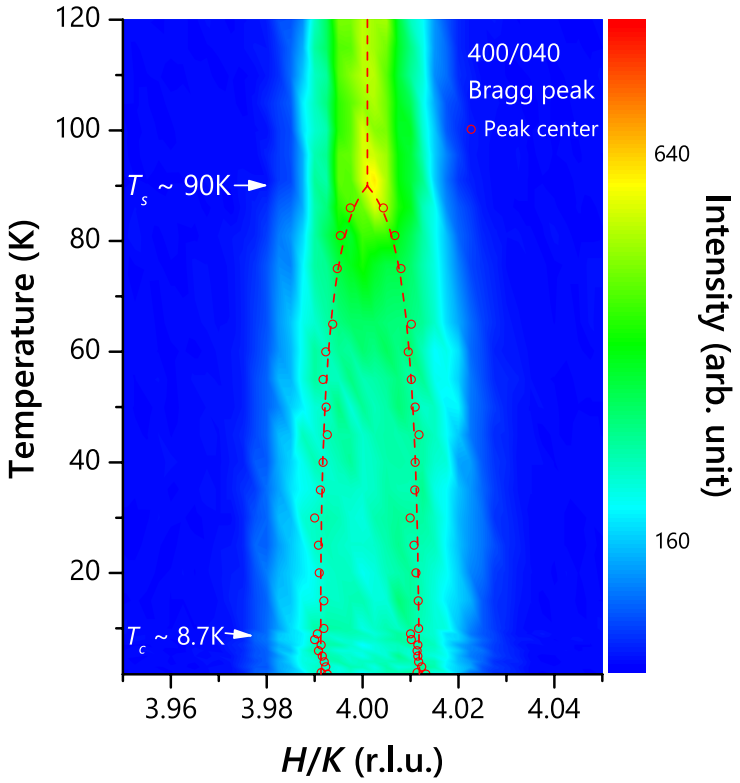

SFig 5: **Temperature dependence of (4, 0, 0)/(0, 4, 0) structure peak**. The 2D contour plot was interpolated from a series of **Q**-scans at different temperatures shown in Fig. 2a. The data were collected on 4F2.